Nanoscale

COMMUNICATION

View Article Online
View Journal | View Issue



Cite this: *Nanoscale*, 2015, **7**, 11951

Received 20th April 2015,
Accepted 4th June 2015

DOI: 10.1039/c5nr02545a

www.rsc.org/nanoscale



# Self-propelled micromotors based on Au–mesoporous silica nanorods†

Ying-Shuai Wang,[a] Hong Xia,*[a] Chao Lv,[a] Lei Wang,[a] Wen-Fei Dong,[a] Jing Feng[a] and Hong-Bo Sun*[a,b]

**Here, a chemical powered micromotor from the assembly of Au–$SiO_2$ nanorods is presented. This new micromotor can be propelled efficiently by hydrogen bubbles generated from a hydrolysis reaction of aqueous $NaBH_4$ and $KBH_4$ and by oxygen bubbles produced by decomposition of $H_2O_2$. The monodisperse Au nanoparticles in mesoporous silica particles could catalyze the decomposition of two different kinds of fuels and produce bubbles. High speeds of 80 μm $s^{-1}$ and recycles of more than 30 times are achieved in both $NaBH_4$ and $H_2O_2$ media. Locomotion and rolling forms of movement were found. The locomotion forms can be obtained in a larger proportion by patterning the Au–$SiO_2$ nanorods and a PDMS membrane. These micromotors that use multiple fuel sources to power them offer a broader scope of preparation and show considerable promise for diverse applications of nanomotors in different chemical environments.**

## 1 Introduction

The automation propulsion of synthetic micro-/nanoscale objects has attracted considerable interest due to their diverse potential practical applications, such as drug delivery, microsurgery, and environment remediation.[1–3] Bubble-propelled micromotors are particularly outstanding owing to their advantages of high energy conversion efficiency, high power output, robust performance, and high motion speed.[4,5] In the field of bubble-powered micro-/nanomotors, Pt is the most common material to generate oxygen gas and create bubbles to propel micromotors forward by means of catalyst catalyzed decomposition of hydrogen peroxide.[6,7] However, the significant cost of Pt catalysts and the requirement of a high-concentration hydrogen peroxide fuel have greatly hindered the practical applications of catalytically propelled micro-/nanomotors.[8] A lot of seminal studies have been looking for alternative catalyst catalyzed materials and fuels. For example, Pumera *et al.* showed an Ag and $MnO_2$-based bubble-powered micromotor.[8] Sen *et al.* have reported a bi-segment Pt/Cu nanowire motor using bromine or iodine fuels.[9] Meanwhile Gao *et al.* showed a hydrogen-bubble-propelled micromotor based on zinc oxidation in an extremely acidic environment.[10] Joseph Wang demonstrated that an Al/Pd Janus micromotor can be propelled in three different fuels: alkali, acid, and hydrogen peroxide.[11] Although these studies are very new and instructive, the oxidation in air of an active metal micromotor, *i.e.* safety and recycling difficulties, and complex fabrication technology obstruct the path to its wide application. A more stable, simple and easily available micromotor propelled in other matrix environments except for hydrogen peroxide is highly desirable.

Gold nanoparticles (Au NPs) have received wide attention in recent years for a variety of catalytic reactions, which is obviously in contrast to the chemical inertness of pure gold films or gold bullion.[12,13] Research studies found that small Au NPs tend to show a higher catalytic activity in a variety of heterogeneous green catalytic processes.[14–17] Therefore, Au NPs can be used as a good candidate to drive part of the micro/nanomotors in specific fuels. However, it is very easy for small Au NPs to aggregate and minimize their surface area due to high surface energy, resulting in a remarkable reduction in their catalytic activities.[14] In this report, high-stability and -reusability Au–$SiO_2$ nanorods are fabricated in which Au nanoparticles are dispersed in one end of mesoporous silica nanorods.

Simple aggregation of Au–$SiO_2$ nanorods is highly efficient in generating bubbles in both borohydride salts (sodium borohydride and potassium borohydride) and hydrogen peroxide solutions, leading to fast bubble-propelled motion of micromotors. Gold-nanoparticles in the range of 2–15 nm are monodispersed in Au–$SiO_2$ nanorods, which ensures that the micromotors have high catalytic activity. Micromotor motion can be propelled by hydrogen or oxygen bubbles generated

[a]*State Key Laboratory on Integrated Optoelectronics, College of Electronic Science and Engineering, Jilin University, 2699 Qianjin Street, Changchun 130012, P.R. China. E-mail: hxia@jlu.edu.cn, hbsun@jlu.edu.cn*

[b]*College of Physics, Jilin University, 119 Jiefang Road, Changchun 130023, P.R. China*

†Electronic supplementary information (ESI) available: More electronic microscopy graphs, UV-Vis spectra and $N_2$ adsorption isotherms. See DOI: 10.1039/c5nr02545a

from two different fuels: sodium borohydride ($NaBH_4$) and hydrogen peroxide ($H_2O_2$) by catalytic decomposition of gold nanoparticles. In particular, micromotors are still capable of moving even when the concentration of $NaBH_4$ solution is low to 0.1 wt%. The average speed can reach 30 μm $s^{-1}$. In the two kinds of fuels, two typical forms of motion, locomotion and rolling, appear. The locomotion forms can be obtained by the Janus Au–$SiO_2$/polydimethylsiloxane (PDMS) microstructure as micromotors from assemblies of Au–$SiO_2$ nanorods on a PDMS membrane and laser ablation processing.

## 2 Experimental details

### 2.1 Materials

Cetyltrimethyl ammonium bromide (CTAB), tetraethyl orthosilicate (TEOS), sodium borohydride ($NaBH_4$) and 4-nitrophenol (4-NP) were purchased from Sigma-Aldrich. Hydrogen peroxide ($H_2O_2$) was purchased from Changchun Bai'ao Trading Co., Ltd. Ammonia and gold chloride acid ($HAuCl_4{\cdot}4H_2O$) were purchased from Beijing Tianyu Technology Co., Ltd. The $HAuCl_4$ solution was kept in the refrigerator for the next step.

### 2.2 Synthesis of the Au–$SiO_2$ nanorod precursor

50 mg of CTAB was dispersed into 10 ml of water and ultrasonicated until clarification. The CTAB solution was poured into a three-necked flask, followed by the addition of amounts of $HAuCl_4$ (0.01 M) solution; then 0.5 ml of ammonia solution was quickly added while the temperature was maintained at 40 °C under stirring. Then 30 μl TEOS was added in. The mixture was kept for 30 min before washing once with methanol to remove parts of excess CTAB and silica gel. Then the precursor was kept in 500 μl water for the next step.

### 2.3 Preparation of aggregations of Au–$SiO_2$ nanorods as micromotors

First, 500 μl Au–$SiO_2$ nanorod precursor solution was added into a glass bottle with a glass slice placed at the bottom. After drying the water at 60 °C, the glass slice with the deposited Au–$SiO_2$ nanorod precursor on the surface was taken out and calcined at 500 °C for 1 h. Au–$SiO_2$ nanorod aggregated layers were formed after cooling to room temperature. The deposited Au–$SiO_2$ nanorod aggregated layers were detached from glass; after a slight concussion in a container the Au catalytic micromotors were obtained.

### 2.4 The preparation of Au–$SiO_2$/PDMS micromotors by laser ablation processing

PVA (polyvinyl alcohol) aqueous solution of 5 wt% was spun on the clean glass slide at a speed of 5000 r $s^{-1}$ to form a PVA membrane; then PDMS was spun on the PVA surface; three minutes later, after drying, the Au–$SiO_2$ nanorods were coated on the surface of PDMS. The composite structure of three layers was kept for 30 min at 90 °C. Then, the multilayered film is ablated by an amplified femtosecond pulse laser in 200 mW and the peak intensity is $2.55 \times 10^{13}$ W $cm^{-2}$ to form a periodic rectangular shape; after soaking in hot water, Au–$SiO_2$/PDMS micromotors were achieved.

## 3 Results and discussion

To obtain the Au-catalyzed and multi-fuel driven bubble-propelled micro/nanomotors, Au–$SiO_2$ nanorods synthesized using a one-pot method as the component of micromotors was selected; the gold nanoparticles in Au–$SiO_2$ nanorods are mono-dispersed and not aggregated. We have determined in our previous work that the Au–$SiO_2$ Janus nanorod catalyst has good catalytic activity and stability in conversion of PNP to PAP in the presence of $NaBH_4$.[18] In the Janus nanorod, gold nanoparticles are dispersed at one end of the mesoporous silica rod that can be used as the driving part, and mesoporous silicon dioxide can be considered as the loading part; thus a "rocket" structure nanomotor with the potential for self-propelling was obtained in this way as shown in Fig. 1(B). But the size of the nanorods with length below 800 nm was too small to be observed, so we prepared more suitable sized micromotors using a self-deposition method.

A schematic diagram of the preparation of bubble-propelled Au catalytic micromotors is shown in Fig. 1(A). At first, we deposit the nanorod precursor on a glass substrate, and anneal the substrate at 500 °C, after cooling, the deposited Au–$SiO_2$ nanorod layer is detached from glass; it is worth noting that in this method, the purification process is different from our previous work, such as reducing the times of purification to leave some silica sol. These differences make it easier for the silica nanorod precursors to adhere to each other, and after annealing, the adhesion of silica makes Au–$SiO_2$ Janus nanorods spontaneously form aggregations with different

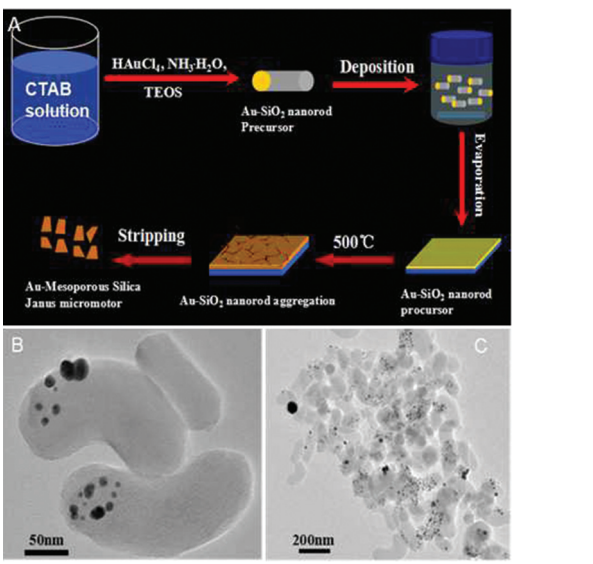


Fig. 1 Schematic diagram of bubble-propelled Au catalytic micromotor preparation (A); (B) TEM image of Au–$SiO_2$ nanorods and (C) TEM image of Au–$SiO_2$ Janus aggregation.

stable structures. TEM of aggregations after they are further broken is shown in Fig. 1(C). An obvious adhesion can be observed between silica nanorods. The aggregations have a good catalytic ability because of the existence of small Au nanoparticles inside the aggregation, and the size of most motors after processing was in the range of 50–150 μm as shown in Fig. S3.† Asymmetry dispersion of gold nanoparticles in the aggregation is the key reason for the aggregation movement; this structure constructed by Au nanoparticles and the adhesion of mesoporous silica was marked as Au–$SiO_2$ micromotors.

We discuss the motion of Au catalyzed bubble-propelled micromotors in an $NaBH_4$ solution through microscope observation. Fig. 2(A) shows the time-lapse images of the movement of an Au catalyzed micromotor in 0.5 wt% $NaBH_4$ aqueous solution with a certain amount of NaOH (see also Video 1†).[19]

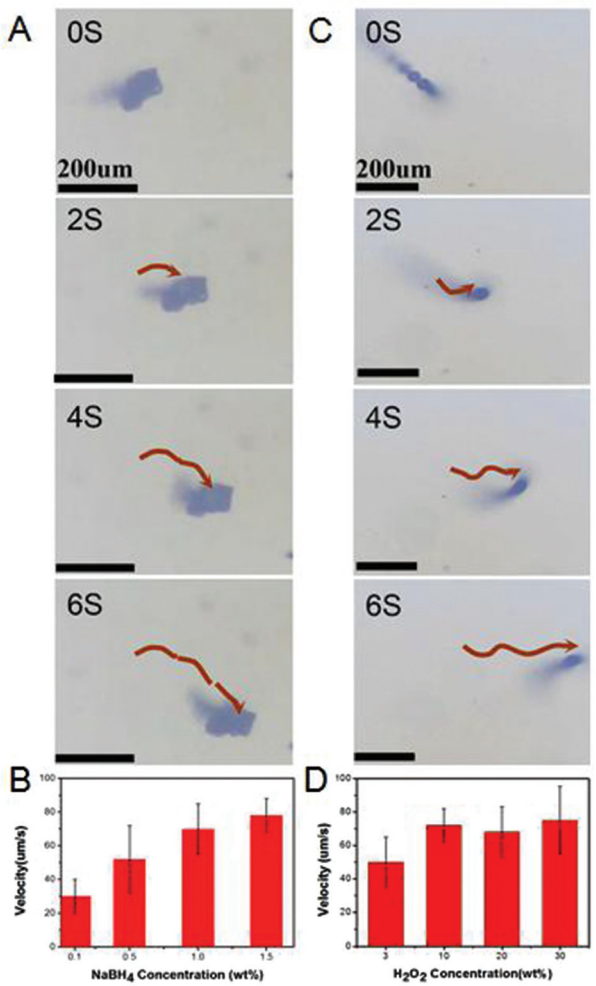


Fig. 2 Motion of bubble-propelled Au catalytic micromotors in different environments. (A) Time-lapse images of Au micromotors in 0.5 wt% $NaBH_4$. (B) Dependence of the average velocity of Au catalytic micromotors on $NaBH_4$ concentration at 20 °C. (C) Time-lapse images of an Au micromotor in 20% $H_2O_2$. (D) Dependence of the average velocity of Au catalytic micro-motors on $H_2O_2$ concentration at 20 °C.

It is worth noting that added NaOH should inhibit the self-hydrolysis of $NaBH_4$. From tracking images for the path of micromotors over a 2 s interval (Fig. 2(A)), continuous hydrogen bubbles were generated by the catalytic decomposition of $NaBH_4$ by Au nanoparticles. The dehydrogenation reaction of $NaBH_4$ can be represented with the following formula:

$$BH_4^- + 2H_2O \rightarrow BO_2^- + 4H_2 \uparrow$$

The hydrogen bubbles are released quickly from the motor as shown in Video 1.† The micromotor was propelled in the opposite direction by hydrogen bubble thrust, and the velocities of the Au–$SiO_2$ micromotors are dependent on the $NaBH_4$ fuel concentration. Fig. 2(B) illustrates the influence of $NaBH_4$ concentration on the average speed of moving Au–$SiO_2$ micromotors. There is an obvious increase in the mobility of Au–$SiO_2$ micromotors with increasing concentration of $NaBH_4$. The micromotors can move at an average speed of ~30 μm $s^{-1}$, even in 0.1 wt% $NaBH_4$, and the average speed of Au catalytic motors exhibiting motion can reach over 80 μm $s^{-1}$ in the presence of 1.5 wt% $NaBH_4$. The percentage of Au motors exhibiting motion and the mobility of the motors also depend on the fuel concentration and the ratio of the size of the Au–$SiO_2$ nanorod aggregates to the Au catalyst. The high bubble frequency reflects the high catalytic efficiency of Au for the decomposition of $NaBH_4$ from Video 1.† For a micro-motor, a nearly constant motion speed was shown under many times recycles based on the advantages of recycling gold catalysts.[20,21] In addition to the given good catalytic performance of Au nanoparticles including high catalytic efficiency and high stability, in the Au–$SiO_2$ nanorod aggregation the mesoporous silica has high load capacity for further potential applications; these reasons imply that the Au–$SiO_2$ nanorod aggregation can be used as good micro-motors.

The motion of micromotors was also observed in $H_2O_2$ as shown in Fig. 2(C). The time-lapse images show the path movement of Au catalyzed micromotors in 20% $H_2O_2$ over a 2 s interval. Oxygen bubbles are generated by the catalytic decomposition of $H_2O_2$ by Au; the $H_2O_2$ decomposition approach can be represented with the following formula:

$$2H_2O_2 \rightarrow 2H_2O + O_2 \uparrow$$

The oxygen bubbles are released from one side of the motor very quickly as shown in Video 2.† The velocity of the Au catalytic motor is dependent on the $H_2O_2$ fuel concentration. Fig. 2(D) illustrates the influence of $H_2O_2$ concentration on the average speed of the moving Au micromotors. There is an increase trend in the mobility of Au micromotors with increasing the $H_2O_2$ concentration. The micromotors can move at an average speed of ~50 μm $s^{-1}$ in 3% $H_2O_2$ and the average speed of Au catalytic motors exhibiting motion can reach over 100 μm $s^{-1}$ in the presence of 30% $H_2O_2$. The high bubble frequency reflects the high catalytic efficiency of Au for the decomposition of $H_2O_2$ from Video 2.† It is interesting that when the concentration of $H_2O_2$ increases by more than 10%, the change of speed of the micromotors is not particularly

steep. We suspect that the reason for this phenomenon is that when the $H_2O_2$ concentration increased to a certain extent, large amounts of oxygen produced by $H_2O_2$ decomposition could not quickly escape from the surface of micromotors to air, and Au nanoparticles were encapsulated in mesoporous silica; the fuel must make contact with Au nanoparticles through pore channels; thereby a large amount of un-escaped oxygen generated by $H_2O_2$ decomposition may block the mesoporous pore channels, and it will affect the rate of catalysis; furthermore it will affect the speed of the movement. It should be mentioned that the micromotors reported here are truly catalytic, and their motion stops only when the fuel is exhausted, and when the fuel is replenished, the motion of the micromotors resumes.

Two typical kinds of model were found for the motion of the Au catalytic micromotors in 0.5 wt% $NaBH_4$ aqueous solutions as shown in Fig. 3: locomotion (A) and rolling (B). We could clearly see from Fig. 3(A) that bubbles escaped from multiple locations of the motor, but the micromotor was moving around in circles, and from Fig. 3(B) we can see that the bubbles quickly escaped from the surface, and the micromotor tumbled violently in the liquid, but the relative position had not changed. The same motion model was also found when the micromotors were kept in 0.5 wt% potassium borohydride ($KBH_4$) as in Fig. 3(C). Similar results were obtained with the micro/nanomotor in 20% $H_2O_2$ and the movement model can also lead to two conditions as shown in Fig. S1:† (A) locomotion and (B) rolling. We could find from Fig. 2(C) and S1† that larger bubbles were generated in $H_2O_2$ compared with the bubbles of $NaBH_4$ and the speed at which bubbles escaped from the surface of the micromotor in $H_2O_2$ was slower; this is related to the basic properties of different gases. Asymmetry is key to the design of micro-/nanomotors;[8] in this work the form of micromotors, movement is related to the morphology, quality and internal distribution of gold nanoparticles. As shown in Fig. S2,† from scanning electron microscopy (SEM) images and energy-dispersive X-ray spectroscopy (EDX) elemental mapping results of bubble-propelled Au catalytic micromotors, we can more clearly see that the distribution of Au nanoparticles in the aggregate structure is uneven; the uneven distribution causes the location of the gases generated by the fuel decomposition to be asymmetric; when bubbles leave the micromotor surface, they can produce different forces on micromotors in different locations; these forces will lead to the movement of micromotors in the fuel.

In order to understand the emergence of the three models, we used a simple model: when the force of the *Z* direction is relatively balanced, and the force in the *X* and *Y* directions uneven, the three-dimensional structure will move in the plane *xoy*, of course, the force of the *Z* axis will change with the formation and disappearance of air bubbles. When the *X*, *Y*, *Z* direction forces are all uneven, the three-dimensional structure cannot lead to a fixed direction motion and rolling will occur. But because the movement of the aggregation is affected by the buoyancy of the liquid and the gas, gravity, surface tension and at the same time the quality distribution of the aggregation are not uniform, *etc*. So in practice the forces of the micromotor are more complex.

In order to obtain locomotion, which is one of the most valuable motions, we fixed Au–$SiO_2$ nanorods to the polymer substrate, and patterned the multilayer membrane structure by femtosecond laser ablation, so that we could obtain the Au–$SiO_2$/PDMS Janus composite structure as micromotors; this structure can even limit the movement of micromotors in a direction through the polymer to limit the catalysis of Au nanoparticles. As shown in Fig. 4(A), at first we spin coated a layer of PVA film which is soluble in water on the glass substrate;[22] after PVA drying, we spun a certain thickness PDMS membrane; when the PDMS membrane was not completely dry, the coverage of Au–$SiO_2$ nanorods on the surface of the PDMS membrane took place; after drying of PDMS, Au–$SiO_2$ nanorods can undergo effective adhesion on the surface of PDMS under the action of gravity. Then, by using the method of laser ablation, through different row spacings, one can obtain different sizes of the rule of PDMS and nanorod composite structures; from the optical microscope image and SEM photos, one can clearly see that the PDMS block structure size

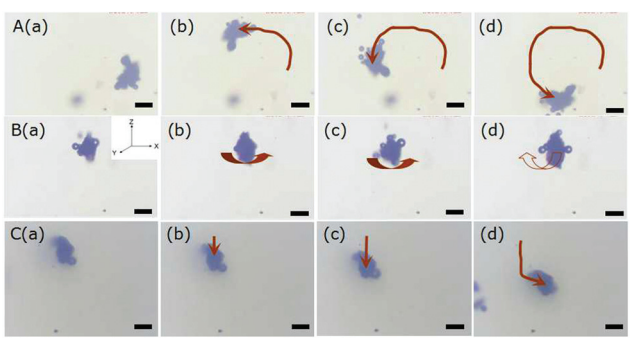


Fig. 3 Different forms of motion of bubble-propelled Au catalytic micromotors in $NaBH_4$ solution (A and B) (0.5 wt%) and in $KBH_4$ (0.5 wt%) (C). The locomotion (A), (C) and rolling (B). The solid line is for Pxoy movement and the hollow one for Pyoz movement. Scale bar: 100 μm.

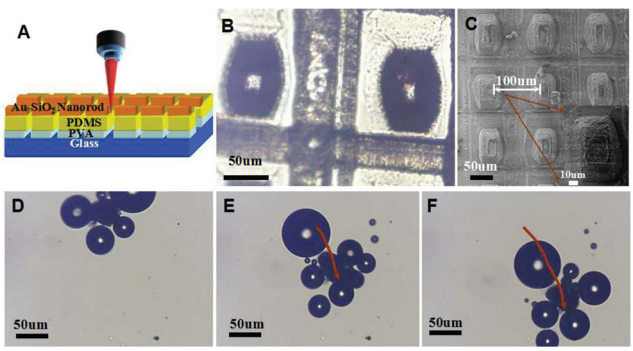


Fig. 4 Diagram image (A), optical microscope photos (B) and scanning electron microscope (SEM) photos (C) of composite structure. (D–F) Time-lapse images of Au micromotors in 10% $H_2O_2$ of composite structure. The interval time is 1 s.

is 50 μm, as shown in Fig. 4(B) and Fig. 4(C). PDMS side roughness increases and a nanostructure appears after laser processing as shown in the inset picture of Fig. 4(C) it improves the surface area and is useful to load drugs or others.

Through the design of the anisotropic PDMS block structure, we can inhibit the gold particles in a certain direction in catalysis to obtain the locomotion of composite structure micromotors as in Fig. 4(D–F), the time-lapse images of Au–$SiO_2$/PDMS micromotors in 10% $H_2O_2$ of composite structure. From Fig. 4(D–F) we can clearly see that rolling is restricted after assembly and composite locomotion along one direction.

In summary, we have presented a new multi-fuel driven bubble-powered micromotor from Au–$SiO_2$ nanorods. These Pt-free, Au based micromotors could be driven by the bubbles from catalytic decomposition of fuels such as hydrogen peroxide and sodium borohydride. The speed of the micromotors can be modulated by changing the concentration of the fuel. Through the polymer pattern we can obtain only locomotion as the micromotor movement. The oxidation resistance, recycling ability, high catalytic activity, and good stability of the Au form (compared to Mg- and Al-based micromotors[23,24]) make an attractive alternative to the currently popular platinum for prolonged propulsion of micro-/nanomotors in a diverse range of practical applications such as in environmental governance, biological fields and others.

## Acknowledgements

This work was supported by 973 Program (grant # 2014CB921302) and the National Natural Science Foundation of China (grant # 61435005, 51335008, 51373064 and 61378053).

## References

1 T. J. Yoon, J. S. Kim and B. G. Kim, *Angew. Chem., Int. Ed.*, 2005, **7**, 1092–1095.
2 P. R. Tardieu and Y. H. Mulet-Marquis, *U.S. Patent*, 4, 482, 1984.
3 W. Gao, X. Feng, A. Pei, *et al.*, *Nanoscale*, 2013, **11**, 4696–4700.
4 A. A. Solovev, S. Sanchez and O. G. Schmidt, *Nanoscale*, 2013, **4**, 1284–1293.
5 L. Soler, V. Magdanz, V. M. Fomin, *et al.*, *ACS Nano*, 2013, **7**, 9611–9620.
6 R. Liu and A. Sen, *J. Am. Chem. Soc.*, 2011, **50**, 20064–20067.
7 S. Sanchez, A. A. Solovev, S. M. Harazim, *et al.*, *J. Am. Chem. Soc.*, 2010, **4**, 701–703.
8 H. Wang, G. Zhao and M. Pumera, *J. Am. Chem. Soc.*, 2014, **7**, 2719–2722.
9 R. Liu and A. Sen, *J. Am. Chem. Soc.*, 2011, **133**, 20064.
10 W. Gao, A. Uygun and J. Wang, *J. Am. Chem. Soc.*, 2011, **134**, 897–900.
11 W. Gao, M. D'Agostino, V. Garcia-Gradilla, J. Orozco and J. Wang, *Small*, 2013, **3**, 467–471.
12 M. Haruta, *CATTECH*, 2002, **6**, 102–115.
13 A. S. K. Hashmi and G. J. Hutchings, *Angew. Chem., Int. Ed.*, 2006, **45**, 7896–7936.
14 B. K. Min and C. M. Friend, *Chem. Rev.*, 2007, **107**, 2709–2724.
15 M. Daniel and D. Astruc, *Chem. Rev.*, 2004, **104**, 293–346.
16 K. E. Peceros, X. Xu, S. R. Bulcock and M. B. Cortie, *J. Phys. Chem. B*, 2005, **109**, 21516–21520.
17 Z. Zhang, C. Shao, P. Zou, *et al.*, *Chem. Commun.*, 2011, **13**, 3906–3908.
18 Y. S. Wang, W. F. Dong, H. Xia, *et al.*, *RSC Adv.*, 2014, **4**, 43586–43589.
19 M. A. López, M. M. Gómez, M. A. Palacios, *et al.*, *Fresenius J. Anal. Chem.*, 1993, **346**, 643–647.
20 J. Zeng, Q. Zhang, J. Chen, *et al.*, *Nano Lett.*, 2009, **10**, 30–35.
21 D. J. Gorin, B. D. Sherry and F. D. Toste, *Chem. Rev.*, 2008, **108**, 3351–3378.
22 C. D. Schaper, *Nano Lett.*, 2003, **3**, 1305–1309.
23 W. Gao, X. Feng, A. Pei, Y. Gu, J. Li and J. Wang, *Nanosacle*, 2013, **5**, 4696–4700.
24 W. Gao, A. Pei and J. Wang, *ACS Nano*, 2012, **6**, 8432–8438.